Journal of Macromolecular Science, Part B
Publication details, including instructions for authors and subscription information:
http://www.informaworld.com/smpp/title~content=t713375300

Dielectric Studies of Segmental Dynamics in Epoxy Nanocomposites

P. Pissis[a]; D. Fragiadakis[a]
[a] Department of Physics, National Technical University of Athens, Athens, Greece

To cite this Article Pissis, P. and Fragiadakis, D.(2007) 'Dielectric Studies of Segmental Dynamics in Epoxy Nanocomposites', Journal of Macromolecular Science, Part B, 46: 1, 119 — 136
To link to this Article: DOI: 10.1080/00222340601044284
URL: http://dx.doi.org/10.1080/00222340601044284

Journal of Macromolecular Science®, Part B: Physics, 46:119–136, 2007

ISSN 0022-2348 print/1525-609X online
DOI: 10.1080/00222340601044284

Dielectric Studies of Segmental Dynamics in Epoxy Nanocomposites

P. PISSIS AND D. FRAGIADAKIS

Department of Physics, National Technical University of Athens, Athens, Greece

Dielectric techniques were employed, along with differential scanning calorimetry (DSC), to investigate segmental dynamics associated with the glass transition in epoxy nanocomposites. Two epoxy network matrices were used, the first based on diglycidyl ether of Bisphenol A (DGEBA) and diethylenetriamine, and the second on DGEBA and poly(oxypropylene)diamine (Jeffamine D2000). In the first matrix, the inclusions were organically modified clays, diamond particles with a diameter of about 6 nm, and conductive carbon nanoparticles with a diameter of about 10 nm, whereas in the second, polyhedral oligomeric silsesquioxanes (POSS) were covalently attached to the chains as dangling blocks. In the nanocomposites of the first matrix, glassy at room temperature, segmental dynamics becomes slower and the glass transition temperature increases on addition of the filler. In the epoxy/POSS nanocomposites, rubbery at room temperature, dynamics is described by a two-phase (layer) model: a fraction of the polymer is immobilized, obviously at interfaces with POSS, whereas the rest is slightly plasticized, compared to the pure matrix.

Keywords epoxy networks, segmental dynamics, glass transition, dielectric spectroscopy, relaxation time, relaxation strength

Introduction

In recent years, organic-inorganic polymer nanocomposites have generated a lot of interest. They may exhibit significant improvement of various properties of the polymer matrix, in particular mechanical properties, thermal stability, and barrier properties, at much lower filler fractions than conventional macroscale or microscale composites.[1–3] Thermoplastic, thermosetting (including epoxy networks), and rubber matrices are used, depending on the application envisaged, whereas nanofillers are often classified in terms of dimensionality: one-dimensional, such as carbon nanotubes, two-dimensional, such as layered silicates (clays), and three-dimensional, such as silica particles.

Molecular dynamics studies in polymer nanocomposites, in particular studies of segmental dynamics and the related glass transition, are interesting from both the fundamental and technological point of view. From the fundamental point of view it is challenging to investigate how chain mobility, relaxation, and thermal transitions, in particular the glass transition of the polymer matrix, are modified by the presence of and interactions

Received 11 July 2006; Accepted 31 July 2006.
In Commemoration of the Contributions of Professor Valery P. Privalko to Polymer Science.
Address correspondence to P. Pissis, Department of Physics, National Technical University of Athens, Zografou Campus, 15780 Athens, Greece. E-mail: ppissis@central.ntua.gr

with the inorganic, typically rigid, fillers. At the same time, modification of chain dynamics by the nanoparticles is at the origin of improvement of several properties which synthesis of polymer nanocomposites aims at, such as thermal stability, mechanical properties, and barrier properties.

Our knowledge of chain dynamics in polymer nanocomposites and, at the same time, our approach to the topic are based on three sources of information: computer simulations, where we typically study how molecular dynamics in a system changes as a function of the distance from a surface;[4,5] measurements in glass forming liquids and polymers confined in model geometries, such as porous glasses and thin films, where we may study effects of interfaces;[6,7] measurements in real polymer nanocomposites, often by combining a variety of experimental techniques.[1–3] Results in real nanocomposites look, at first glance, controversial and confusing: dynamics (often quantified in terms of glass transition temperature) may become faster or slower or show no change, it may be homogeneous or heterogeneous, and so on.[8] We may bring some order into these results and explain many of them by considering two contradictory effects of nanoparticles on chain dynamics:[9] dynamics may become slower, in particular close to interfaces, due to constraints imposed to the motion of the chains by the rigid nanoparticles, this effect being more pronounced in the case of covalent bonds between the two components (hybrid organic–inorganic nanocomposites); at the same time, dynamics may become faster as a result of increase of free volume due to loosened molecular packing of the chains (plasticization).

Results may become more complex in thermoset nanocomposites, including epoxy network nanocomposites, as compared to nanocomposites based on thermoplastic and rubber matrices. The reason for this is that curing reactions and crosslinking density may be modified by the presence of the nanofillers or the matrix may be plasticized by smaller molecules present in the network.[10,11] This "secondary" effect should be distinguished from the "primary" one of direct influence of the nanofillers on chain dynamics.

Results obtained with epoxy layered silicate nanocomposites have recently been reviewed.[10] Both, a constant or increased glass transition temperature T_g and a reduction of T_g with increasing organoclay addition have been reported. Sun et al.[12] studied several epoxy nanocomposites with various inclusions (silica, silver, aluminum, carbon black) and observed a depression of T_g, related with enhanced polymer dynamics due to extra free volume at the resin-filler interface. Miyagawa et al.[13] observed a slight increase of T_g in epoxy/clay nanocomposites (by 1.5°C at 6 vol. %). It is interesting to note in this connection that dynamic mechanical analysis (DMA) measurements in phenolic-based cyanate ester/clay nanocomposites indicated a significant increase of T_g and broadening of the response.[14] The morphology of the epoxy/clay nanocomposites (intercalation vs. exfoliation) proved to be significant for the effect on T_g.[15,16] Effects of water on thermal transitions in epoxy/clay nanocomposites were studied by Becker et al.[17] Lu and Nutt[18] investigated the relaxation behavior of epoxy/clay nanocomposites by a combination of standard and temperature modulated differential scanning calorimetry (DSC). Addition of the intercalated nanoparticles resulted in a slower overall relaxation, a wider distribution of relaxation times, and higher T_gs. A domain relaxation model was proposed that included three possible relaxation modes.[18]

In the present work we employ dielectric techniques (broadband dielectric relaxation spectroscopy—DRS and thermally stimulated depolarization currents—TSDC) to investigate the segmental dynamics associated with the glass transition in epoxy nanocomposites. The broad frequency range of dielectric techniques allows us to study in detail the dynamic glass transition over a wide temperature range.[19] A variety of nanocomposites prepared using two different matrices, one based on DGEBA-diethylenetriamine and the other on DGEBA-Jeffamine, and various fillers, including organically modified clays, diamond,

carbon, and POSS nanoparticles, were studied and results obtained with the various systems were critically compared to each other.

Dielectric techniques have already been used to study various epoxy nanocomposites. Sun et al.[12] observed high values of both real and imaginary part of the dielectric function, ε' and ε'', in epoxy nanocomposites with various fillers. Nelson and Fothergill[20] investigated epoxy/TiO_2 nanocomposites at low frequencies where conductivity and space charge polarization dominate the response. Todd and Shi[21] pointed to the effects of coupling agent on the interface dielectric constant. Qi et al.[22] followed percolation in epoxy/Ag nanocomposites in terms of ε' vs. vol. % and pointed to the prospects of such nanocomposites as high ε' materials.

Experimental

Materials

Two epoxy network matrices were used, the first based on a low-viscosity epoxy resin (ER), diglycidyl ether of Bisphenol A (DGEBA, Araldite LY556, Ciba) and diethylene-triamine as curing agent, and the second on DGEBA and poly(oxypropylene)diamine (Jeffamine D2000, molar mass 2000). In the first matrix the inclusions were smectic clays organically modified with three quaternized ammonium salts: SAN (Hexadecyl, octadecyl ammonium chloride), STN (Trioctane-, methyl-ammonium chloride), and SPN (Oligo(oxypropylene)-, diethyl-, methyl-ammonium chloride);[23,24] diamond particles synthesized by a shock-wave method with a diameter of about 6 nm;[25] conductive nanosized carbon particles (NCP) synthesized by a shock-wave method with a diameter of about 10 nm.[26] In the second matrix, the inclusions were DGEBA-based polyhedral oligomeric silsesquioxane (POSS) monomers with cyclopentyl substituents, covalently attached to the chains as dangling blocks.[27,28] Details of the preparation of the nanocomposites and of structural and morphological characterization have been given in the above references.[23–28]

Techniques

DSC measurements were carried out using a Perkin-Elmer DSC-4 calorimeter.

A Schlumberger Frequency Response Analyzer (FRA SI 1260) supplemented by a buffer amplifier of variable gain (Chelsea Dielectric Interface) or a Novocontrol Alpha Analyzer, both in combination with a Novocontrol Quatro Cryosystem, were used for DRS measurements in the frequency range $10^{-2} - 10^{6}$ Hz. Measurements in the frequency range 10^{6}–10^{9} Hz were carried out using a Hewlett-Packard impedance/material analyzer (4291A) integrated with a Tabai Espec temperature chamber (SU-240-Y).

The TSDC method consists of recording the thermally activated release of frozen-in polarization.[8] A Novocontrol sample cell designed for TSDC was used, in combination with a Novocontrol Quatro System and a Keithley 617 electrometer.

Results and Discussion

Epoxy/Diamond Nanocomposites

Figure 1 shows results for the frequency dependence of the dielectric permittivity $\varepsilon = \varepsilon' - i\varepsilon''$ for the nanocomposite with 1.2 vol. % diamond at temperatures between

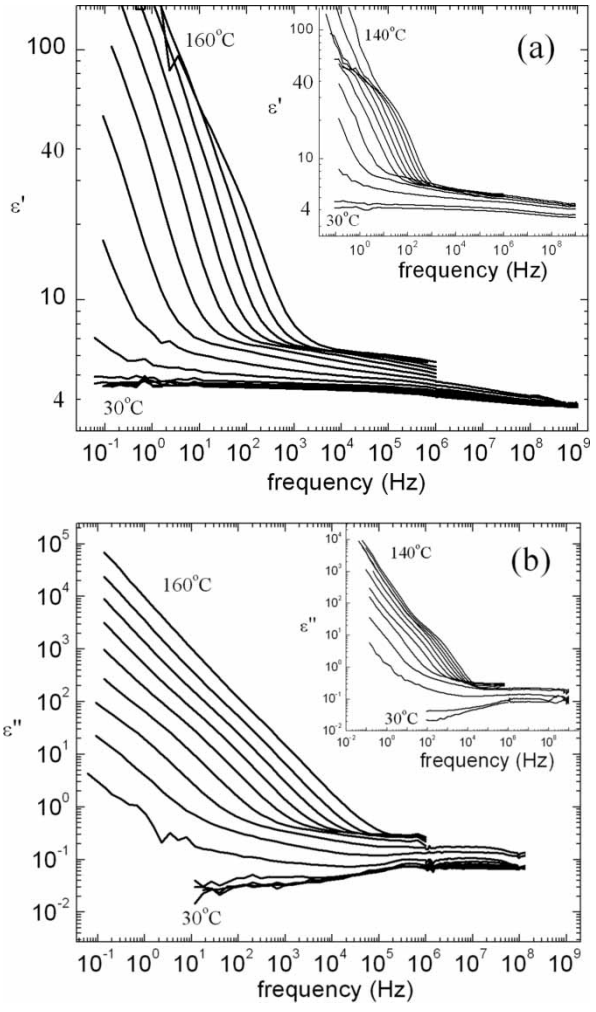

Figure 1. Log-log plot of the real (a) and imaginary (b) part of the dielectric permittivity for the 1.2% epoxy/diamond nanocomposites at various temperatures, in steps of 10°C. The insets show the corresponding plots for the epoxy matrix.

30 and 160°C and a broad frequency range from 10^{-1} to 10^{6} Hz, extended for some temperatures to 10^{9} Hz. For direct comparison, the inset shows the corresponding plots for the ER matrix. We observe high values of ε' and ε'' at low frequencies and high temperatures. Also, a step is observed in ε' at low frequencies and high temperatures and a corresponding shoulder in ε'', both more pronounced in the pure ER matrix (in the temperature range 100–130°C) than in the nanocomposite. All these observations are related to DC conductivity and conductivity effects,[23,25] which will not be further discussed here. The results are not very conclusive with respect to the segmental α relaxation, corresponding to the glass transition (dynamic glass transition). The main reason for this is that the corresponding loss peak in Fig. 1 is masked by conductivity. However, we observe a large increase of $\varepsilon'(f)$ for the pure ER (inset to Fig. 1) between 40 and 50°C, which suggests an increase in molecular mobility in this temperature range. This indicates that the glass transition of the

epoxy network takes place between 40 and 50°C. This increase is observed in the nanocomposite at higher temperatures, 70–100°C, and is much more gradual. These results are confirmed by comparative isochronal (constant frequency) $\varepsilon'(T)$ plots at selected high frequencies (to eliminate conductivity effects) not shown here.

The shift of the α relaxation and of the glass transition to higher temperatures in the diamond nanocomposites with respect to the pure ER matrix is more clearly observed in the isochronal $\varepsilon''(T)$ plot of Fig. 2. The α loss peak at the frequency of representation of 10^5 Hz in Fig. 2 is shifted from about 90°C in the pure ER matrix to about 130°C in the two diamond nanocomposites. Two more points are of particular interest here; the first being that the whole α loss peak is shifted to higher temperatures in the nanocomposites and secondly, there is no indication for a second loss peak located at the temperature of the α loss peak in the pure matrix. Thus, with respect to the ongoing discussion in the literature about the effects of the nanoparticles on segmental dynamics and glass transition of the polymer matrix,[8,10] the results in Fig. 2 indicate that in the diamond nanocomposites these effects are not limited to a surface layer around the nanoparticles. On the contrary, the molecular mobility of the whole matrix is (severely) restricted in the nanocomposites. The second point refers to the observation that the shift to higher temperatures and the shape of α loss peak is the same for the two nanocomposites, despite the different content of nanoparticles (0.5 against 1.2%), which results in a different mean distance between the particles of 13 and 18 nm, respectively.[25]

Despite the strong contribution of conductivity and space charge polarization to the $\varepsilon'(f)$ and $\varepsilon''(f)$ data in Fig. 1, the dynamics of the α relaxation could be analyzed. It is possible, under certain conditions, for a relaxation where the $\varepsilon''(f)$ loss peak is completely masked by DC conductivity, to eliminate the conductivity contribution by calculating by a derivative method $\varepsilon''(f)$ from the measured $\varepsilon'(f)$, where DC conductivity makes no contribution.[29] We followed that method and calculated $\varepsilon''(f)$ for the ER matrix and the nanocomposites at selected temperatures, where the contribution of DC conductivity to $\varepsilon'(f)$ appeared negligible (60–150°C for the ER matrix,

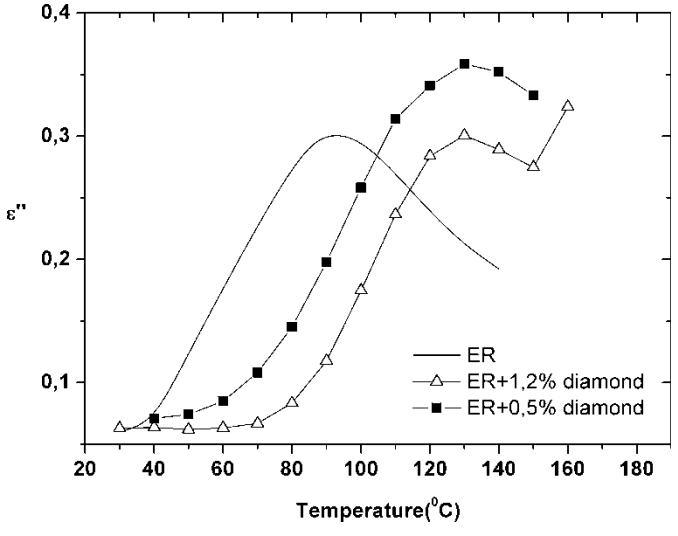

Figure 2. Dielectric loss ε'' against temperature for ER/diamond nanocomposites indicated on the plot at 10^5 Hz.

115–130°C for the nanocomposite with 0.5% diamond, and 90–140°C for the nanocomposite with 1.2% diamond), by[29]

$$\varepsilon''_{\mathrm{der}} = -\frac{\pi}{2}\frac{\partial\varepsilon'(\omega)}{\partial \ln(\omega)} \approx \varepsilon''_{\mathrm{rel}} \tag{1}$$

where $\omega = 2\pi f$. As an example Fig. 3 shows comparative measured and calculated $\varepsilon''(f)$ plots for the nanocomposite with 1.2% diamond at three temperatures. The frequency of the maximum of the dielectric loss $f_{\max}$ for the α relaxation was obtained from the calculated spectra at each temperature and is plotted in the Arrhenius diagram (activation diagram) of Fig. 4. The temperature dependence of $f_{\max}$ is well described by the Vogel-Tammann-Fulcher equation[30]

$$f_{\max} = A\exp\left(-\frac{B}{T - T_0}\right) \tag{2}$$

where A, B, and T_0 (Vogel temperature) are temperature independent empirical constants. The α relaxation is significantly slower in the nanocomposites as compared to the matrix; note, however, that doubling the volume fraction of the filler from 0.5% to 1.2% seems to only slightly affect the dynamics. The glass transition temperatures indicated by DRS measurements, calculated by extrapolating the data in Fig. 4 to a relaxation time of 100 s (equivalent frequency of 1.6×10^{-3} Hz),[8,30] are 47°C for the pure ER, and about 80°C for the nanocomposites.

Thus, both the isochronal $\varepsilon''(T)$ results in Fig. 2 and the results shown in the Arrhenius plot, obtained independently from each other (in the sense that the former were obtained from the measured $\varepsilon''(f)$, whereas the latter from the $\varepsilon'(f)$ data), show a significant restriction of segmental dynamics and a significant increase of glass transition temperature T_g in the nanocomposites, as compared to pure matrix. Such changes in T_g are often discussed in terms of a layer of polymer with reduced mobility (bound polymer) around the filler particles, with a thickness of the order of a few nm (two- or three-layer models[8,10,18]). When the interparticle distance becomes comparable to the thickness of this interfacial layer, it will constitute a large volume fraction of the overall material and its properties

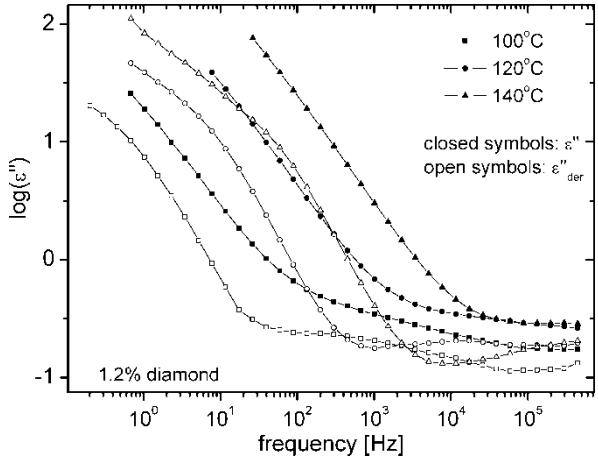

Figure 3. Comparative measured (ε'') and calculated ($\varepsilon''_{\mathrm{der}}$) dielectric loss against frequency for the nanocomposite with 1.2 vol. % diamond at selected temperatures indicated on the plot.

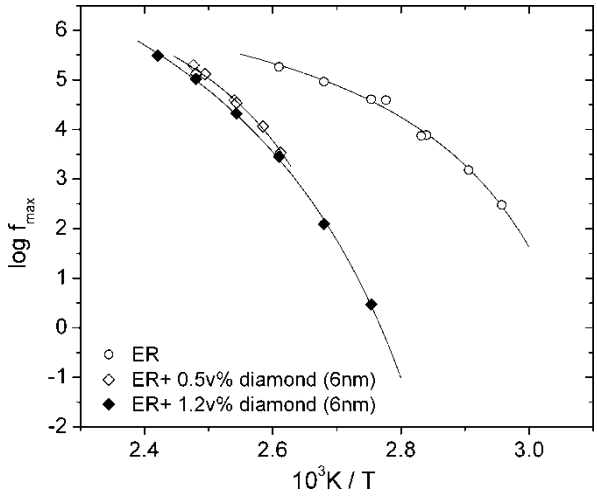

Figure 4. Arrhenius plot for the α relaxation of the epoxy/diamond nanomposites indicated on the plot. The lines are fits of the VTF Eq. (2).

will dominate the bulk properties of the material. The interparticle distances here, however, are much larger than typical values obtained for the thickness of the interfacial layer found in the literature (a few nm[8]), even assuming that the particles have been completely dispersed in the matrix. It can not be excluded, however, that curing of the polymer in the presence of the nanoparticles (the method of preparation followed here) has a direct influence on the structure and the properties of the matrix.

Epoxy/Clay Nanocomposites

Transmission electron microscopy studies (TEM) indicated that, in the ER/clay nanocomposites studied, the clays were mostly exfoliated.[23] Results for the temperature dependence of $\varepsilon'(T)$ and of $\varepsilon''(T)$ in the clay nanocomposites in a broad temperature region around T_g are given in Figs. 5 and 6, respectively. The samples contain 5 wt. % organically modified clays.[23] We assume, at this stage, that changes observed in the dielectric spectra on addition of clay reflect changes in the morphology and the dynamic of the epoxy network and that the quaternized ammonium salts used for clay modification make no direct contribution to the dielectric spectra.[21] Similar to the case of diamond nanocomposites, isothermal results of $\varepsilon'(f)$ and $\varepsilon''(f)$ are not very conclusive with respect to the segmental α relaxation. A high frequency (10^5 Hz) was selected for the isochronal plots to eliminate conductivity and space charge polarization.

The step in $\varepsilon'(T)$ at around 60°C in pure ER in Fig. 5 and at higher temperatures in the nanocomposites corresponds to the dynamic glass transition. This interpretation is based on the well-established fact that molecular dipoles which are frozen in the glassy state and, thus, do not contribute to ε', become mobile and contribute to ε' in the rubbery state. Interestingly, $\varepsilon'(T)$ is constant in ER at $T > T_g$, whereas in the nanocomposites it continues to increase with increasing temperature, indicating a gradual release of constraints to chain mobility imposed by the rigid nanoparticles. The α loss peak in Fig. 6 is at about 90°C in pure ER and is shifted, by about 20–40°C, to higher temperatures in the nanocomposites, whereas at the same time it becomes less clear, in correlation with the gradual release of

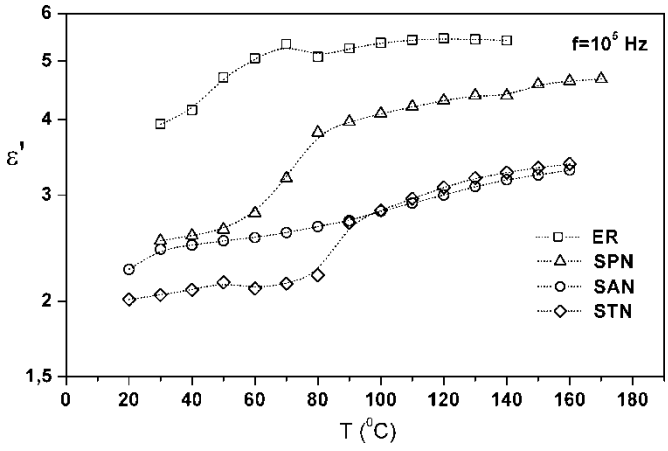

Figure 5. Real part of the dielectric permittivity ε' against temperature T of the ER/clay nanocomposites indicated on the plot at 10^5 Hz.

frozen mobility at higher temperatures indicated by the results in Fig. 5. Obviously, the (calorimetric) T_g is located at a lower temperature than the α loss peak in Fig. 6 because of the high frequency of presentation in Fig. 6.[30]

Thus, the results of dielectric studies in the ER-clay nanocomposites clearly indicate restriction of segmental dynamics in the nanocomposites, as compared to the pure matrix. The quality of dielectric data, in particular the large contribution of conductivity and of space charge polarization to ε' and ε'', precludes from discussing the data in terms of a model. It is interesting to note, however, that the results in Figs. 5 and 6, in agreement with those presented in the previous section for epoxy/diamond nanocomposites, appear incompatible with any model where a significant part of the polymer in the nanocomposites exhibits segmental dynamics similar to that of the pure matrix.

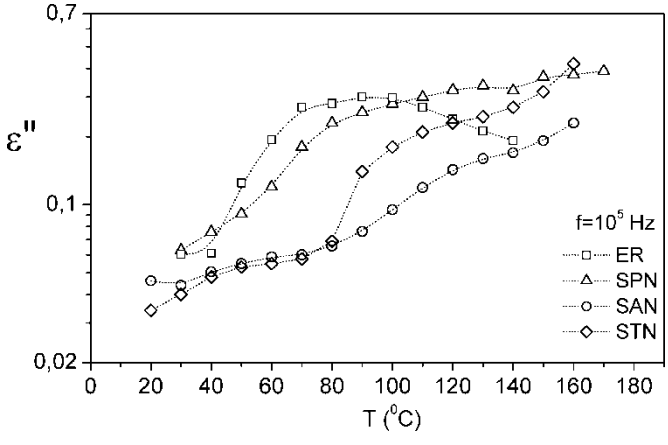

Figure 6. Dielectric loss ε'' against temperature T of the ER/clay nanocomposites indicated on the plot at 10^5 Hz.

Epoxy/Carbon Nanocomposites

This is a system of particular interest, as the filler is conductive and the results of dielectric studies can be discussed in terms of percolation and, thus, provide additional information on morphology. From the technological point of view such systems are interesting for applications as high ε' materials and as conducting polymers ("light metals") below and above the percolation threshold, respectively.[22,26]

Molecular dynamics in the nanocomposites was studied by broadband DRS and TSDC. Figure 7 shows results for the temperature dependence of ε' and ε'' in the ER/NCP nanocomposites at a constant frequency of 80,805 Hz, whereas comparative TSDC thermograms of the pure matrix and three nanocomposites are given in Fig. 8. The TSDC thermograms correspond to plots of dielectric loss against temperature $\varepsilon''(T)$ at a fixed low frequency in the range 10^{-2}–10^{-4} Hz.[8] The three ER/NCP nanocomposites have filler volume fractions Φ of 1, 4, and 6%, all three below the percolation threshold, which was determined from a plot of ε' (at a fixed frequency of 1 Hz and a temperature of -50°C) against Φ to be 7.4%.[26] An overall increase of molecular mobility is observed in Figs. 7 and 8, in the sense that, at each temperature, ε' and ε'', as well as the depolarization current, increase with increasing filler content. This is, to a large extent, related to the formation of a percolation structure of the nanoparticles.

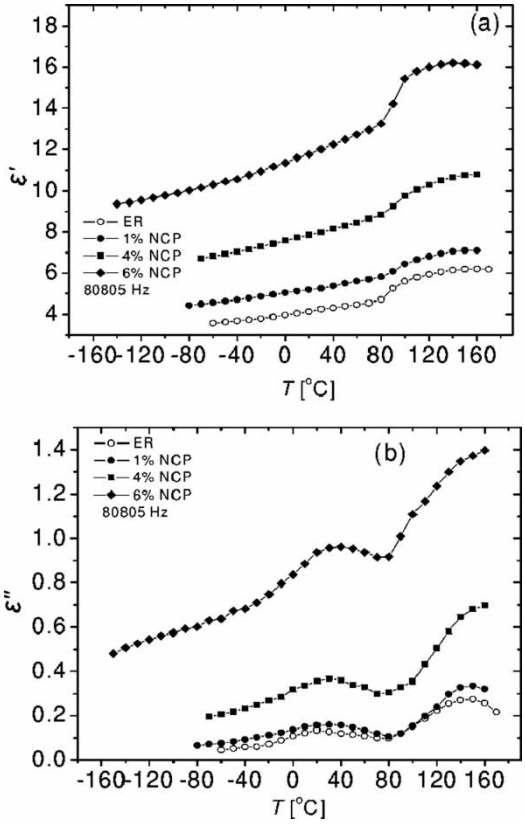

Figure 7. Temperature dependence of the real ε' (a) and the imaginary part (dielectric loss) ε'' (b) of the dielectric permittivity of the ER/carbon nanocomposites indicated on the plot at 80,805 Hz.

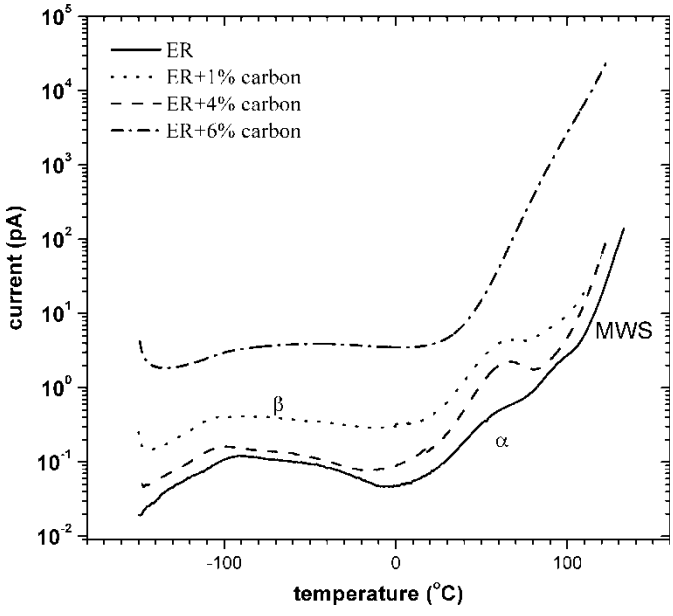

Figure 8. TSDC thermograms for the ER/carbon nanocomposites indicated on the plot.

Two relaxations, a secondary β relaxation at lower temperatures, associated with the motion of hydroxyl groups[31] and the segmental α relaxation at higher temperatures, associated with the glass transition of the ER matrix, are observed in Fig. 7. For both relaxations the strength (i.e., the magnitude of the peak in $\varepsilon''(T)$ and the corresponding step in $\varepsilon'(T)$) increases in the nanocomposites, in particular for the sample with the highest Φ value. The time scale (temperature position) of the response shows, however, a different behavior for the two relaxations: no change for the local β relaxation against a shift to higher temperatures, i.e., a slowing down of dynamics, with increasing filler content for the segmental α relaxation. Similar results (even if less conclusive) are obtained by TSDC (Fig. 8), where in addition to the β and the α relaxations an interfacial Maxwell-Wagner-Sillars (MWS) relaxation[29] is observed in the ER matrix at higher temperatures (interestingly, however, not in the nanocomposites). The α relaxation in Fig. 8 is recorded as a shoulder on the steeply increasing wing of depolarization current arising from conductivity. Please note the logarithmic current scale, as well as the fact that the β relaxation is superimposed on a background, which also increases significantly with increasing filler content and is attributed to interfacial polarization within the clusters formed by association of the carbon particles.

Thus, the results of DRS and of TSDC in the ER/NCP nanocomposites allow discussing molecular mobility in terms of the relaxation strength and the time scale of the response. The increase of relaxation strength for the α relaxation, as well as for the β relaxation, can be understood in terms of increased free volume, in agreement with results obtained with other nanocomposites.[9] The slowing down of the cooperative α relaxation (dynamic glass transition), on the other hand, is in agreement with the results obtained with the same matrix and different inclusions (clays and diamond nanoparticles) in the two previous sections.

Epoxy/POSS Nanocomposites

The chemical structures of the materials used for preparation, DGEBA, Jeffamine D2000 and the DGEBA-based POSS monomer with cyclopentyl substituents, $POSS_{cp\text{-}DGEBA}$, and of the networks prepared are shown in Scheme 1. Along with the pure epoxy network (sample d), two hybrids were investigated, samples d_1 and d_2, both with dangling POSS blocks covalently attached to the chains, differing in the weight fraction of POSS units, 35% and 50%, respectively. The crosslinking density was kept constant in the three samples.[27,28]

The glass transition in the pure network and the hybrids was studied by DSC, the results (second runs to delete any effects of thermal history) being listed in Table 1, glass transition temperature, T_g, determined as the temperature of half heat capacity increase, range of the glass transition, ΔT, determined as the difference between the temperature of completion, and the temperature of onset of the glass transition, heat capacity jump at T_g, ΔC_p, and heat capacity jump normalized to the polymer fraction in the hybrids, ΔC_{pn}, determined by $\Delta C_{pn} = \Delta C_p/(1 - w)$, where w is the weight fraction of the POSS unit.

T_g in Table 1 is in the range of about $-45^{\circ}C$, i.e., the epoxy networks prepared are in the rubbery state at room temperature. T_g shows no systematic variation with composition; however, a significant and systematic broadening with increasing weight fraction of POSS is

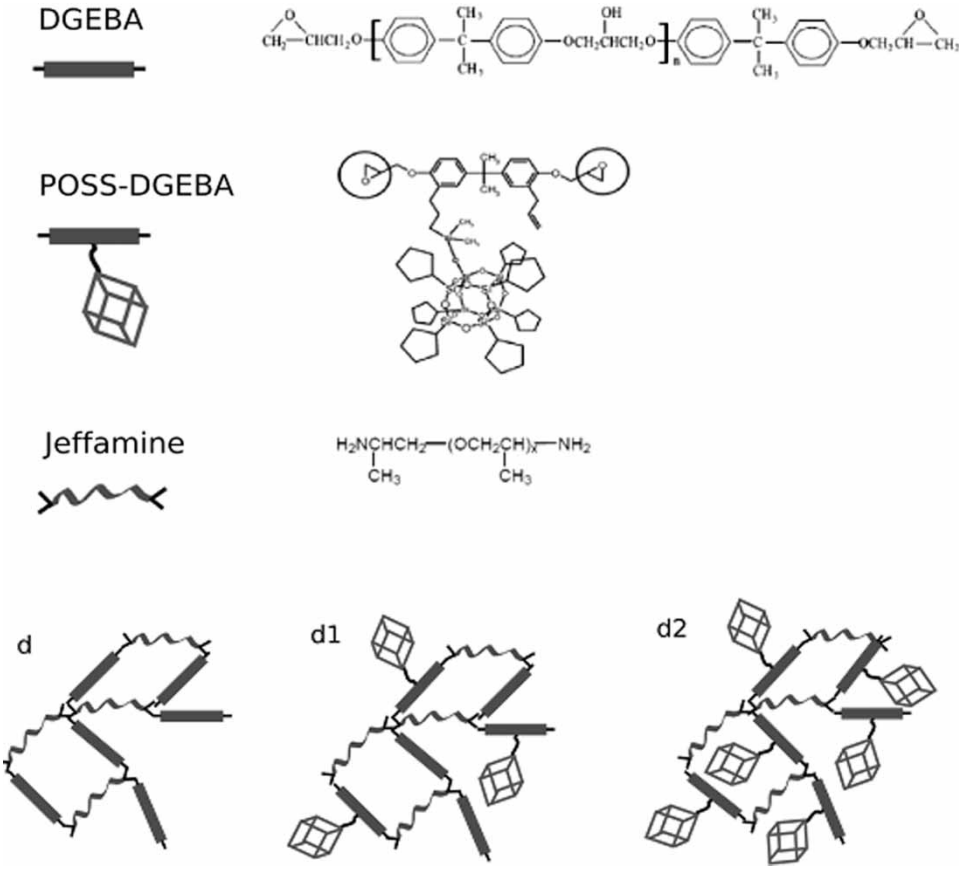

Scheme 1. Chemicals used and structure of the materials studied.

observed. Also, the heat capacity jump at T_g, normalized to the same polymer fraction, ΔC_{pn}, is approximately the same for the three samples studied. The broadening of the response in the region of the glass transition, confirmed also by TSDC results, not shown here, and by DMA results on the same samples,[28] suggest increasing heterogeneity of chain dynamics at the glass transition, i.e., chain dynamics is different in different regions of the sample. The characteristic size of these regions must be larger than the characteristic length (cooperativity length) of the glass transition, which has been determined for various polymers to be in the range 1–4 nm.[30] The spatial heterogeneity in the hybrids can be understood in terms of the two main effects caused by the presence and the covalent bonding of the POSS units:[9] increase of free volume due to loosened molecular packing of the chains and constraints imposed to the motion of the chains by the rigid particles.

DRS measurements (10^{-2}–10^6 Hz) were carried out isothermally from −150 to 150°C. The broad frequency and temperature ranges allow following all the relaxations present in the samples, dipolar relaxations at lower temperatures/higher frequencies, and relaxations related with charge carrier motion at higher temperatures/lower frequencies. An overview of the dielectric response is given in the isochronal $\varepsilon''(T)$ plot of Fig. 9. A low frequency of 10 Hz has been chosen for that plot in order to follow, in a single plot, all the relaxations present in the pure epoxy network and the hybrids: the local, secondary γ and β relaxations in the glassy state, the segmental α relaxation, and the normal mode (NM) relaxation in the temperature region of the glass transition, DC conductivity and conductivity effects at higher temperatures. The NM relaxation is characteristic for chains having a dipole moment component along the chain contour, arising from the fluctuation and orientation of the end-to-end polarization vector of the chain in the electric field.[32,33] Jeffamine, having a dipole moment component along the chain contour, is the origin of the NM relaxation in the nanocomposites under investigation. Here we focus on the two relaxations in the glass transition region. Please note that ε'' in Fig. 9 has been normalized to the same polymer fraction, $\varepsilon''_{norm} = \varepsilon''/(1 - w)$, where w is the weight fraction of the POSS units, so that the magnitudes of the relaxations (heights of the loss peaks) in the various samples can be directly compared to each other, by assuming, at this stage, that only the polymer fraction contributes to the relaxations observed. The most striking result in Fig. 9 is the significant reduction of the normalized response in the region of the glass transition in the hybrids, as compared to the pure epoxy network, in agreement also with TSDC results not shown here. Before we proceed with the analysis of the data, by fitting appropriate model functions to $\varepsilon(f)$ data, we would like to extract more information on the time scale and the magnitude of the relaxations solely on the basis of the raw data.

Figure 10 shows comparative $\varepsilon''(f)$ plots of the three samples under investigation at −20°C, to follow the segmental relaxation and the NM relaxation. The double peak shifts slightly to higher frequencies with increasing POSS content in the hybrids,

Table 1
Glass transition characteristics of the epoxy/POSS nanocomposites

Sample	T_g (°C)	ΔT (°C)	ΔC_p (J/g°C)	ΔC_{pn} (J/g°C)
d	−44	25	0.75	0.75
d1	−48	42	0.54	0.83
d2	−43	70	0.36	0.72

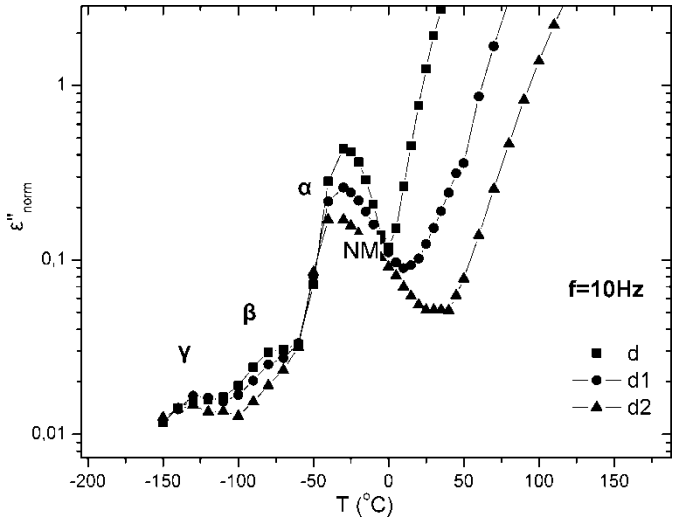

Figure 9. Comparative isochronal $\varepsilon''(T)$ plot of the epoxy/POSS nanocomposites indicated on the plot at 10 Hz.

indicating an acceleration of the response in the region of the glass transition. Also, the magnitude of the relaxations decreases significantly in the hybrids, as shown also by the normalized $\varepsilon''(T)$ plots in Fig. 9. Both the segmental α relaxation and the NM relaxation in our networks originate from Jeffamine, as indicated by comparison with dielectric data obtained with linear and star poly(oxypropylene).[32] A striking result in Fig. 10, by comparing with these dielectric data,[32] is the relatively very strong contribution of the NM relaxation to the double peak. It is well known from the theory that the relaxation strength of the NM relaxation increases with the square of chain length (end-to-end polarization vector of the chain). Measurements in poly(oxybutylene) (B) oligomers of various molar masses and in block copolymers of poly(oxybutylene) and poly(oxyethylene) (E), EB and EBE, where the E blocks are crystalline and the B blocks amorphous, have shown that, at each molar mass of the B block, the normalized relaxation strength of the NM relaxation of the B blocks increases significantly in the diblocks and even more in the triblocks, as compared to the homopolymers.[33] These results have been explained by assuming that the B blocks in the block copolymers are more expanded and oriented, in agreement with the results of structural studies.[33] Thus, the results in Fig. 10 suggest that Jeffamine, the origin of the NM relaxation in our epoxy networks, is stretched in the networks, in agreement with and in support of a structure model of the networks proposed on the basis of SAXS, WAXS, and TEM measurements.[27] The model involves a lamellar structure with POSS crystalline layers separated by extended Jeffamine D2000 chains.

The dielectric data were further analyzed by fitting appropriate model functions to the measured spectra. Based on previous experience,[8,19] a sum of two Havriliak-Negami (HN) expressions of the type[34]

$$\varepsilon(\omega) = \varepsilon_\infty + \frac{\Delta\varepsilon}{(\mathbf{1} + (i\omega i_{HN})^{\mathbf{1}-a})^\beta} \tag{3}$$

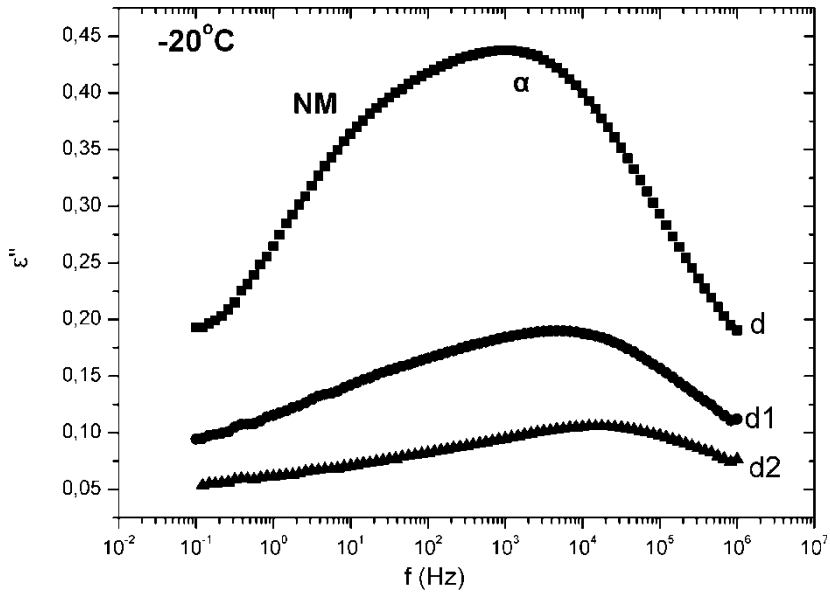

Figure 10. Comparative $\varepsilon''(f)$ plot of the epoxy/POSS nanocomposites indicated on the plot at -20°C.

was fitted, at each temperature, to the dielectric spectra in the region of the double α-NM peak. In this expression, $\varepsilon^* = \varepsilon' - i\varepsilon''$ is the complex dielectric permittivity (function), $\omega = 2\pi\tau$, $\Delta\varepsilon$ the intensity (magnitude, strength) of the relaxation process, $\tau_{HN} = 1/(2\pi f_{\mathrm{HN}})$ and f_{HN} the position of the relaxation process on the frequency scale, ε_∞ is $\varepsilon'(f)$ for $f \gg f_{\mathrm{HN}}$ and α and β are shape parameters. For each of the two relaxations, α and NM, the frequency of maximum loss (peak frequency) $f_{\max}$ was calculated by[35]

$$f_{\max} = f_{\mathrm{HN}}\left[\frac{\sin[((1-a)\pi/(2+2\beta))]}{\sin[((1-a)\beta/(2+2\beta))]}\right]^{1/(1-\alpha)} \tag{4}$$

By the fitting procedure described above, information extracted from each relaxation is quantified in terms of time scale ($f_{\max}$), magnitude ($\Delta\varepsilon$), and shape (α, β) of the response. In the following we focus on the information on time scale and magnitude of the two relaxations in the temperature region of the glass transition.

Time scale is best discussed in terms of the Arrhenius plot (activation diagram) shown in Fig. 11 for the three samples studied. Included in the plot are also TSDC data at the equivalent frequency of 1.6×10^{-3} Hz, corresponding to a relaxation time of 100 s,[8] in very good agreement with the DRS data. We observe in Fig. 11 that both the segmental α relaxation and the NM relaxation become faster with increasing POSS content in the hybrids. The two relaxations approach each other with decreasing temperature toward T_g, as expected for oligomers[32,33] and is clearly observed for the pure epoxy network, the sample with the larger response. Please note that this closer merging of the two relaxations, as the cooperativity length (characteristic length) of the glass transition[30] increases toward the chain length of Jeffamine, combined with the reduction of the response in the hybrids (Fig. 10), makes results of the analysis more ambiguous, in particular for the weaker NM relaxation. The VTF Eq. (2) was fitted to the data for the α and NM

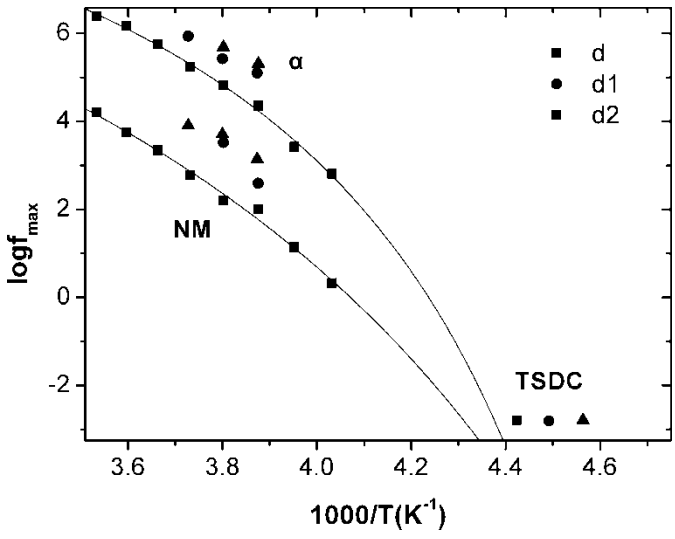

Figure 11. Arrhenius plot for the two relaxations and the three samples indicated on the plot. Included are also TSDC data. The lines are fits of the VTF Eq. (2) to the data for the pure epoxy network.

relaxations only for the pure epoxy network sample, where more data were available, with reasonable values of the fitting parameters (log A = 11.8, B = 1071 K, T_0 = 196.7 K for α and log A = 12.4, B = 2115 K, T_0 = 171 K for the NM relaxation).

Thus, the results of broadband DRS show clearly, in agreement with the TSDC results, that the segmental α relaxation and the NM relaxation become slightly but systematically faster in the hybrids with increasing POSS content, as compared to the pure epoxy network. The corresponding reduction of T_g, from the TSDC data which are included in Fig. 11, is 3 and 7°C for the samples with 35 and 50 wt. % POSS units, respectively, as compared to the pure epoxy network. The acceleration of the α and the NM relaxations in the hybrids may be explained in terms of an increase of free volume, arising from loosened molecular packing of the chains due to the presence of the rigid and bulky POSS units and their covalent bonding to the chains. Plasticization by the bulky POSS units[36] is a different terminology for the same effect. A significant increase of free volume, confirmed also by density measurements, has been observed in polyimide networks modified by POSS units.[37]

The relaxation strength of each of the two relaxation processes, obtained from the fitting of the HN expression as shown in Eq. (3) to the experimental data, was normalized to the same mass fraction of the polymer, $\Delta\varepsilon_n = \Delta\varepsilon/(1 - w)$, where w is the mass fraction of the POSS units. $\Delta\varepsilon_n$ was plotted as a function of temperature for each of the processes. The plots, not shown here, reveal, as expected from the literature,[19] a decrease of $\Delta\varepsilon_n$ with increasing temperature for the segmental α relaxation. What is unexpected is the observed clear increase of $\Delta\varepsilon_n$ with increasing temperature for the NM relaxation, as it is well established that for homopolymers $\Delta\varepsilon_n$ decreases with increasing temperature, even faster than $\Delta\varepsilon_n$ for the segmental α relaxation.[33] This increase may be related with the structure ordering found in DGEBA-Jeffamine networks[38] and a disordering at higher temperatures, also suggested by the results of DMA measurements.[28]

Mean values of $\Delta\varepsilon_n$, over the temperature range of measurements, were found to decrease with increasing POSS content in the hybrids for both relaxation processes: $\Delta\varepsilon_n = 2.35$, 1.53, and 1.09 for α and $\Delta\varepsilon_n = 1.83$, 1.70, and 0.75 for the NM relaxation in the order d, d_1, and d_2. These results quantify the significant reduction of $\Delta\varepsilon_n$ of the segmental α relaxation and of the NM relaxation in the hybrids, already observed in Figs. 9 and 10. A possible explanation for this behavior, consistent with the results on time scale of the relaxations, is that a significant part of the chains is immobilized due to the presence of and interactions with the rigid POSS units, whereas the rest exhibits a slightly faster dynamics, as compared to the pure network.

Conclusion

Dielectric techniques (broadband DRS and TSDC, a special technique in the temperature domain) were employed, in addition to DSC, to investigate segmental dynamics associated with the glass transition in epoxy nanocomposites. Two epoxy network matrices were used, the first based on DGEBA and diethylenetriamine, and the second on DGEBA and Jeffamine D2000. In the first matrix, the inclusions were organically modified clays, diamond particles with a diameter of about 6 nm, and conductive carbon nanoparticles with a diameter of about 10 nm, whereas in the second polyhedral oligomeric silsesquioxanes (POSS) were covalently attached to the chains as dangling blocks. Common to the nanocomposites of the first matrix is that no covalent bonds exist between the matrix and the filler. The nanocomposites of the first matrix are glassy at room temperature, whereas the epoxy/POSS nanocomposites are rubbery.

Jeffamine, the diamine used for preparing the epoxy/POSS nanocomposites, possesses a dipole moment component along the chain contour and, thus, exhibits, in addition to the segmental α relaxation associated with the glass transition, a NM relaxation, associated with the fluctuation and orientation of the end-to-end polarization vector of the chain in the electric field. The existence of this relaxation provides additional possibilities for studying chain dynamics by dielectric techniques.

In all the nanocomposites studied, the results show a significant increase of heterogeneity of dynamics in the region of the glass transition, as compared to the pure epoxy network, which reflects a spatial heterogeneity.

In the nanocomposites based on the first epoxy network the segmental dynamics becomes slower, as compared to the pure epoxy network, and the glass transition temperature increases (to an extent depending on the type of inclusion and increasing in the order carbon nanoparticles, clays, diamond nanoparticles). There is neither a fraction of polymer immobilized nor a fraction exhibiting dynamics similar to that of the pure epoxy network. Thus, the results suggest that the dynamics of the whole polymer fraction is influenced by the presence of the nanofiller, even at low filler content.

Results are different in the nanocomposites based on the second epoxy network (epoxy/POSS nanocomposites). A fraction of polymer is immobilized, obviously at interfaces with POSS, whereas the rest exhibits a slightly faster dynamics, as compared to the pure epoxy network. Interestingly, immobilization is clearly observed by both dielectric techniques, however, not by DSC. Thus, polymer dynamics in the epoxy/POSS nanocomposites is described by a two-phase (layer) model. Two- and three-phase models have been used before to describe polymer dynamics in polymer nanocomposites, in particular rubber/silica nanocomposites.[8,39]

At this stage we can only speculate about the reasons for the different behavior in the two classes of nanocomposites studied. Immobilization of a part of the matrix and faster

dynamics for the rest of the matrix in the epoxy/POSS nanocomposites may originate from covalent bonding and the bulky shape of the POSS particles, respectively. On the other hand, the single behavior of the whole polymer in the nanocomposites of the second class may be related with the rigidity of that network. It is also possible that the different behavior of the two classes of nanocomposites originate from the different methods of preparation: the crosslinking density is kept constant in the epoxy/POSS nanocomposites,[27] whereas in the first class of nanocomposites it can not be excluded that curing reactions and crosslinking density may be modified by the presence of the nanofillers or the matrix may be plasticized by smaller molecules present in the network.[10,11] Obviously, more systematic work by varying type and topology of the filler is needed to further clarify these points.

References

1. Alexandre, M.; Dubois, P. Polymer-layered silicate nanocomposites: preparation, properties and uses of a new class of materials. Mater. Sci. Eng. **2000**, *28*, 1.
2. Sanchez, C.; Soler-Illia, C.J. de A.A.; Ribot, F.; Lalot, T.; Mayer, C.R.; Cabuil, W. Designed hybrid organic-inorganic nanocomposites from functional nanobuilding blocks. Chem. Mater. **2001**, *13*, 3061.
3. Ray, S.S.; Okamoto, M. Polymer/layered silicate nanocomposites: a review from preparation to processing. Prog. Polym. Sci. **2003**, *28*, 1539.
4. Starr, F.W.; Schroeder, T.B.; Glotzer, S.C. Molecular dynamics simulation of a polymer melt with a nanoscopic particle. Macromolecules **2002**, *35*, 4481.
5. Scheidler, P.; Kob, W.; Binder, K. The relaxation dynamics of a supercooled liquid confined by rough walls. J. Phys. Chem. B **2004**, *108*, 6673.
6. Barut, G.; Pissis, P.; Pelster, R.; Nimtz, G. Glass transition in liquids: two versus three-dimensional confinement. Phys. Rev. Lett. **1998**, *80*, 3543.
7. Alcoutlabi, M.; McKenna, G.B. Effects of confinement on material behavior at the nanometere size scale. J. Phys. Condensed Matter **2005**, *17*, R461.
8. Fragiadakis, D.; Pissis, P.; Bokobza, L. Glass transition and molecular dynamics in poly(dimethylsiloxane)/silica nanocomposites. Polymer **2005**, *46*, 6001.
9. Bershtein, V.A.; Egorova, L.M.; Yakushev, P.N.; Pissis, P.; Sysel, P.; Brozova, L. Molecular dynamics in nanostructured polyimide-silica hybrid materials and their thermal stability. J. Polym. Sci. Part B Polym. Phys. **2002**, *40*, 1056.
10. Becker, O.; Simon, G.P. Epoxy layered silicate nanocomposites. Adv. Polym. Sci. **2005**, *179*, 29.
11. Valentini, L.; Armentano, I.; Puglia, D.; Kenny, J.M. Dynamics of amine functionalized nanotubes/epoxy composites by dielectric relaxation spectroscopy. Carbon **2004**, *42*, 323.
12. Sun, Y.; Zhang, Z.; Moon, K.-S.; Wong, C.P. Glass transition and relaxation behavior of epoxy nanocomposites. J. Polym. Sci. Part B Polym. Phys. **2004**, *42*, 3849.
13. Miyagawa, H.; Rich, M.J.; Drzal, L.T. Amine-cured epoxy/clay nanocomposites. I. Processing and chemical characterization. J. Polym. Sci. Part B Polym. Phys. **2004**, *42*, 4384.
14. Ganguli, S.; Dean, D.; Jordan, K.; Price, G.; Vaia, R. Chemorheology of cyanate ester organically layered silicate nanocomposites. Polymer **2003**, *41*, 6901.
15. Ellis, T.S.; D'Angelo, J.S. Thermal and mechanical properties of a polypropylene nanocomposite. J. Appl. Polym. Sci. **2003**, *90*, 1639.
16. Kinloch, A.J.; Taylor, A.C. Mechanical and fracture properties of epoxy/inorganic micro- and nanocomposites. J. Mater. Sci. Lett. **2003**, *22*, 1439.
17. Becker, O.; Varley, R.J.; Simon, G.P. Thermal stability and water uptake of high performance epoxy layered silicate nanocomposites. Eur. Polym. J. **2004**, *40*, 187.
18. Lu, H.; Nutt, S. Restricted relaxation in polymer nanocomposites near the glass transition. Macromolecules **2003**, *36*, 4010.

19. Runt, J.P.; Fitzgerald, J.J. (Eds.) *Dielectric Spectroscopy of Polymeric Materials*; American Chemical Society: Washington, DC, 1997.
20. Nelson, J.K.; Fothergill, J.C. Internal charge behavior of nanocomposites. Nanotechnology **2004**, *15*, 586.
21. Todd, M.G.; Shi, F.G. Characterizing the interphase dielectric constant of polymer composite materials: Effect of chemical coupling agent. J. Appl. Phys. **2003**, *94*, 4551.
22. Qi, L.; Lee, B.I.; Chen, S.; Samuels, W.D.; Exarhos, G.J. High-dielectric-constant silver-epoxy composites as embedded dielectrics. Adv. Mater. **2005**, *17*, 1777.
23. Kanapitsas, A.; Pissis, P.; Kotsilkova, R. Dielectric studies of molecular mobility and phase morphology in polymer-layered silicate nanocomposites. J. Non-Cryst. Solids **2002**, *305*, 204.
24. Kotsilikova, R. Processing-structure-properties relationships of mechanically and thermally enhanced smectite/epoxy nanocomposites. J. Appl. Polym. Sci. **2005**, *97*, 2499.
25. Fragiadakis, D.; Pissis, P.; Elie, C.; Kanapitsas, A.; Kotsilkova, R.; Stavrev, S.; Nedkov, I. Dielectric studies of interfacial phenomena in polymer nanocomposites. Proc. 10th International Conference on Mechanics and Technology of Composite Materials, Sofia, Bulgaria, September 2003.
26. Kotsilkova, R.; Fragiadakis, D.; Pissis, P. Rheinforcement effect of carbon nanofillers in an epoxy resin system: Rheology, molecular dynamics, and mechanical studies. J. Polym. Sci. Part B Polym. Phys. **2005**, *43*, 522.
27. Matejka, L.; Strachota, A.; Plestil, J.; Whelan, P.; Steinhart, M.; Slouf, M. Epoxy networks reinforced with polyhedral oligomeric silsesquioxanes (POSS). Structure and morpholofy. Macromolecules **2004**, *37*, 9449.
28. Strachota, A.; Kroutilova, I.; Kovarova, J.; Matejka, L. Epoxy networks reinforced with polyhedral oligomeric silsesquioxanes (POSS). Thermomechanical properties. Macromolecules **2004**, *37*, 9457.
29. Van Turnhout, J.; Wuebbenhorst, M. Analysis of complex dielectric spectra. II. Evaluation of the activation energy landscape by differential sampling. J. Non-Cryst. Solids **2002**, *305*, 50.
30. Donth, E. *The Glass Transition: Relaxation Dynamics in Liquids and Disordered Materials*; Springer: Berlin, 2001.
31. Mijovic, J.; Zhang, H. Local dynamics and molecular origin of polymer network-water interactions as studied by broadband dielectric relaxation spectroscopy, FTIR, and molecular simulations. Macromolecules **2003**, *36*, 1279.
32. Nicolai, T.; Floudas, G. Dynamics of linear and star poly(oxypropylene) studied by dielectric spectroscopy and rheology. Macromolecules **1998**, *31*, 2578.
33. Kyritsis, A.; Pissis, P.; Mai, S.-M.; Booth, C. Comparative dielectric studies of segmental and normal mode dynamics of poly(oxybutylene) and poly(oxyethylene)-poly(oxybutylene) diblock copolymers. Macromolecules **2000**, *33*, 4581.
34. Havriliak, S., Jr.; Havriliak, S.J. *Dielectric and Mechanical Relaxation in Materials*; Hanser: Munich, 1997.
35. Diaz-Calleja, R. Comment on the maximum of the loss permittivity for the Havriliak-Negami equation. Macromolecules **2000**, *33*, 8924.
36. Pielichowski, K.; Njuguna, J.; Janowski, B.; Pielichowski, J. Polyhedral oligomeric silsesquioxanes (POSS)-containing nanohybrid polymers. Adv. Polym. Sci. **2006**, *201*, 225.
37. Lee, Y.-J.; Huang, J.-M.; Kuo, S.-W.; Lu, J.-S.; Chang, F.-C. Polyimide and polyhedral oligomeric silsesquioxane nanocomposites for low-dielectric applications. Polymer **2005**, *46*, 173.
38. Beck Tan, N.C.; Bauer, B.J.; Plestil, J.; Barnes, D.J.; Liu, D.; Matejka, L.; Dusek, K.; Wu, W.L. Network structure of bimodal epoxies – a small angle X-ray scattering study. Polymer **1999**, *40*, 4603.
39. Tsagaropoulos, G.; Eisenberg, A. Dynamic-mechanical study of the factors affecting the 2 glass-transition behavior of filled polymers–similarities and differences with random ionomers. Macromolecules **1995**, *28*, 6067.